A Series of Multicolor Electrochromic Ruthenium(II) Trisbipyridine Complexes: Synthesis and Electrochemistry

François Pichot,† Jeffrey H. Beck, and C. Michael Elliott*

Department of Chemistry, Colorado State University, Fort Collins, Colorado 80523

Received: April 12, 1999; In Final Form: May 28, 1999

A series of 5,5′-disubstituted 2,2′-bipyridines and their corresponding tris complexes with ruthenium(II) have been synthesized. The substituents used (ketone, ester, nitrile, imide, and two amides) are all electron withdrawing in nature and, with one exception, contain a carbonyl group in the position α to the bipyridine ring. The reduction potentials of the free ligands and ruthenium complexes have been determined by cyclic voltammetry and are correlated with the Hammett σ constants of the substituents. Finally, the electron-withdrawing nature of these substituents shifts the reduction potentials of each complex sufficiently positive that up to six stable ligand-based reductions are observable. In these reduced oxidation states, all of the complexes display multicolor electrochromism.

Introduction

Trisbipyridineruthenium(II) complexes possess very rich photochemical and electrochemical properties which have been exploited in both applied and fundamental ways.[1−3] In one particular instance,[4a] the complex $[Ru(L_1)_3]^{2+}$, where L_1 is 5,5′-bis(ethoxycarbonyl)-2,2′-bipyridine, displays distinctly different absorption spectra for each accessible oxidation state (formal states +2 through −4). The specific spectral changes result in a vivid multicolor electrochromism which could potentially find applications in display devices. Interestingly, while the complex having analogous ester substitution in the 4- and 4′-positions exhibits similar electrochemistry, it lacks the pleasing electrochromism.[4b] Also, electron-donating substituents (in either the 5- or 4-position of substitution) do not produce multicolor electrochromism; moreover, they decrease the number of reduced oxidation states accessible within the typical electrochemical solvent window.[5] This study focuses on the effect that several electron-withdrawing functional groups located in the 5- and 5′-positions of the bipyridine have on the electrochemistry of the ligands and on the electrochromic properties of their tris complexes with ruthenium. Furthermore, the relationship between the redox potentials of the ligand and the Hammet constant for the substituents is considered.

Experimental Section

Generalities about the Syntheses of Ligands and Complexes. All the ligands prepared were 2,2′-bipyridines substituted in the 5- and 5′-positions with electron-withdrawing functions. The first step in each synthesis involved the transformation of the 5,5′-dicarboxylicacid (5COOHBp) into the corresponding diacid chloride (5COClBp). In a typical preparation, 1−2 g of 5COOHBp was combined with a large excess of thionyl chloride (100 to 200 mL) and allowed to reflux under nitrogen until the mixture became translucent. After an additional hour of reflux ensuring completion of the reaction, the thionyl chloride was removed by rotary evaporations and the product was dried under vacuum. Due to the reactive nature of the acid chloride, no further purification was attempted and the acid chloride was used for the next step immediately after drying.

Synthesis of 5,5′-Bis(ethoxycarbonyl)-2,2′-bipyridine: L_1. This ligand was prepared as previously described.[4a]

Synthesis of 5,5′-Bis(diethylamido)-2,2′-bipyridine: L_2. A large excess (>20 equiv) of diethylamine was combined with 5COClBp in a refluxing mixture (1:1 V/V) of acetonitrile and dichloromethane for 12 h under nitrogen. After rotary evaporation of the solvent, the product was redissolved in dichloromethane, washed with a solution of sodium carbonate in water, and separated from impurities by liquid chromatography (silica gel; 1:1 ethyl acetate/dichloromethane). The yield was nearly quantitative. MS: $m/z = 354.3$ (parent molecule). ^{1}H NMR δ in ppm from TMS, $CDCl_3$ (multiplicity, integration): 1.1(bs, 3H); 1.3(bs, 3H); 3.3(bs, 2H); 3.6(bs, 2H); 7.9(d, 1H); 8.5(d, 1H); 8.7(s, 1H).

Synthesis of 5,5′-Di(*N*-methyl-*N*-phenylamido)-2,2′-bipyridine: L_3. The same reaction conditions as for L_2, replacing diethylamine with *N*-methylaniline, were used. The product, L_3, was separated from polar impurities by liquid chromatography (silica gel, ethyl acetate) and recrystallized from ethyl acetate. The yield was nearly quantitative. MS: $m/z = 422.2$ (parent molecule). ^{1}H NMR δ in ppm from TMS, $CDCl_3$ (multiplicity, integration): 3.5(s, 3H); 7.1(m, 2H); 7.3(m, 3H); 7.7(d, 1H); 8.1(d, 1H); 8.5(s, 1H).

Synthesis of 5,5′-Dicyano-2,2′-bipyridine: L_4. In a typical preparation, 200 mg of 5COClBp was dissolved in 200 mL of warm dichloromethane. This solution was added dropwise over a period of 30 min to a vigorously stirred aqueous solution (300 mL) of ammonium hydroxide (approximately 0.5 M). Upon the addition, the primary amide formed precipitates. After the addition was completed, the white precipitate was filtered, washed with water, and dried overnight under vacuum. This amide was then ground into a fine powder and allowed to react with a large excess of refluxing thionyl chloride, which acts as a dehydrating agent,[6] under nitrogen for 24 h. After rotary evaporation of the thionyl chloride, the product was purified by liquid chromatography (silica gel, ethyl acetate). The yield was typically less than 40%. MS: $m/z = 206.1$ (parent

* Corresponding Author.
† Present address: National Renewable Energy Laboratory, 1617 Cole Blvd., Golden, CO 80401.

10.1021/jp991196w CCC: $18.00
Published on Web 07/16/1999

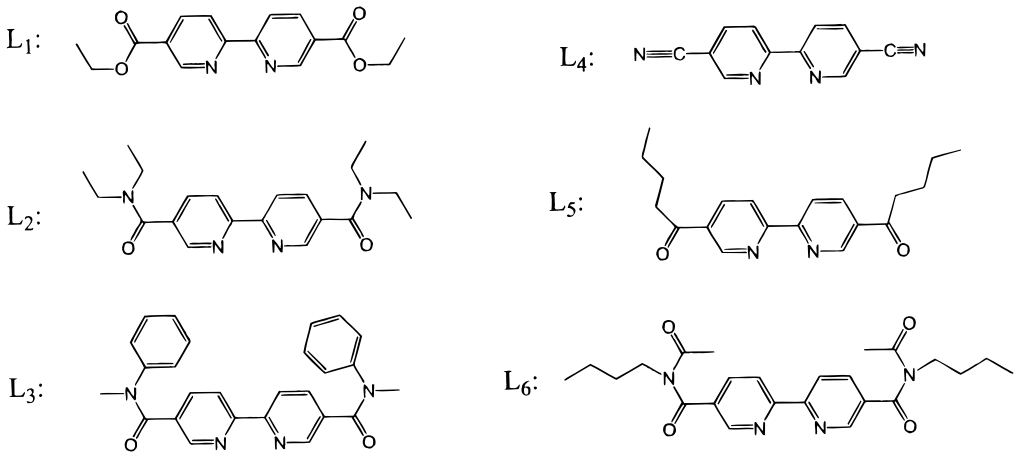

Figure 1. Structures of the substituted 2,2′-bipyridines used in this study.

molecule). ^{1}H NMR δ in ppm from TMS, $CDCl_3$ (multiplicity, intregation): 8.1(d, 1H); 8.6(d,1H); 9.0(s, 1H).

Synthesis of 5,5′-Di(1-ketobutyl)-2,2′-bipyridine: L_5. This compound was synthesized via an adapted literature preparation.[7] Typically, 0.5 g of 5COClBp was added to 3 equiv of $(n\text{-Bu})_2$CuLi in THF at −78 °C under argon. After an hour at this temperature, the solution was slowly warmed to room temperature and subsequently quenched with water. After rotary evaporation of the THF, the product was extracted with ethyl acetate and separated from impurities by liquid chromatography (silica gel, ethyl acetate). The ketone was further purified by recrystallization from ethyl acetate. Overall yield = 15%. MS: m/z = 325.41 (protonated parent molecule). ^{1}H NMR δ in ppm from TMS, $CDCl_3$ (multiplicity, integration): 1.0(t, 3H); 1.4-(m, 2H); 1.8(m, 2H); 3.0(t, 2H); 8.3(d, 1H); 8.6(d, 1H); 9.2(s, 1H).

Synthesis of 5,5′-Di((*N*-(ethan-1-one)-*N*-butylimide)-2,2′-bipyridine: L_6. In a typical preparation, 200 mg of 5COClBp was dissolved in 200 mL of warm dichloromethane. This solution was added dropwise to a large excess of *n*-butylamine dissolved in water (200 mL 0.5 M). The primary amide formed immediately precipitated. This white precipitate was filtered, washed with water, and dried overnight under vacuum. After it was ground into a fine powder, this amide was allowed to react with a large excess of refluxing acetyl chloride under nitrogen. After solvent rotary evaporation, the final product was purified by liquid chromatography (silica gel, 1:1 ethyl acetate/dichloromethane) and recrystallized from cyclohexane. Yield = 60%. MS: m/z = 439.33 (protonated parent molecule). ^{1}H NMR δ in ppm from TMS, $CDCl_3$ (multiplicity, integration): 0.7(t, 3H); 1.2(m, 2H); 1.5(m, 2H); 2.2(s, 3H); 3.7(t, 2H); 8.0(d, 1H); 8.4-(d, 1H); 8.7(s, 1H).

The structures of the previously synthesized ligand (L_1) and of the newly synthesized ligands (L_2, L_3, L_4, L_5, and L_6) are presented in Figure 1.

Synthesis of $[Ru(L_1)_3](PF_6)_2$, $[Ru(L_2)_3](PF_6)_2$, $[Ru(L_3)_3](PF_6)_2$, and $[Ru(L_4)_3](PF_6)_2$. These complexes were all synthesized in the same way. Between 30 and 70 mg of $Ru(DMSO)_4Cl_2$ was added to 2−4 mL of ethylene glycol in a 25 mL round-bottom flask and quickly brought to reflux until the solution became orange. The solution was then immediately cooled to 120 °C, whereupon 3.3 equiv of ligand (L_1, L_2, L_3, or L_4) were added. After completion of the reaction (as determined by TLC), the solution was cooled to room temperature and diluted with 10−15 mL of water. Upon addition of 1−2 mL of saturated aqueous NH_4PF_6, the final product precipitates as the hexafluorophosphate salt. After filtration of this precipitate, the desired complex was isolated by liquid chromatography (silica gel, 1:1 acetonitrile/aqueous 0.02 M KNO_3). After rotary evaporation of the acetonitrile, the complex was reprecipitated as the hexafluorophosphate salt, filtered, washed with water, and dried under vacuum. The ruthenium source was $RuCl_3 \cdot 3H_2O$. The reaction mixture was heated to 160 °C in a sealed Pyrex tube for 18 h.

Synthesis of $[Ru(L_5)_3](PF_6)_2$. The solvent used for this synthesis was DMF, as ethylene glycol yielded a mixture of products, presumably due to the formation of ketals and hemiketals on the bipyridine substituents.

$[Ru(L_2)_3](PF_6)_2$. ^{1}H NMR δ in ppm from TMS, $CDCl_3$ (multiplicity, integration): 1.0(bs, 3H); 1.2(bs, 3H); 3.8(bs, 2H); 4.1(bs, 2H); 7.6 (s, 1H); 8.1(d, 1H); 8.6(d, 1H). UV−visible (wavelength (nm), ϵ/ϵ_{MLCT}): 224 (2.3); 256 (2.8); 305 (5.7); 440 (0.8); 470 (1).

$[Ru(L_3)_3](PF_6)_2$. ^{1}H NMR δ in ppm from TMS, $CDCl_3$ (multiplicity, integration): 3.3(s, 3H); 7.0(m, 2H); 7.2(m, 3H); 7.5(s, 1H); 7.8(d, 1H); 8.2(d, 1H). UV−visible (wavelength (nm), ϵ/ϵ_{MLCT}): 210 (8.3); 306 (7.1); 447 (0.7); 480 (1).

$[Ru(L_4)_3](PF_6)_2$. ^{1}H NMR δ in ppm from TMS, $CDCl_3$ (multiplicity, integration): 8.0(s, 1H); 8.2(d, 1H); 8.8(1H). UV−visible (wavelength (nm), ϵ/ϵ_{MLCT}): 256 (5.2); 298 (10.4); 460 (0.8); 502 (1).

$[Ru(L_5)_3](PF_6)_2$. ^{1}H NMR δ in ppm from TMS, $CDCl_3$ (multiplicity, integration): 1.1(t, 3H); 1.5(m, 2H); 1.9(m, 2H); 2.9(t, 2H); 3.6(bm, 6H); 7.9(s, 1H); 8.2(d, 1H); 8.7(d, 1H). UV−visible (wavelength (nm), ϵ/ϵ_{MLCT}): 226 (3.4); 268 (3.6); 310 (9); 465 (0.8); 502 (1).

Attempted Synthesis of $[Ru(L_6)_3](PF_6)_2$. Attempts at synthesizing this complex under a variety of conditions were unsuccessful.

Electrochemistry of the Free Ligands and Corresponding Ruthenium Complexes. Tetra-*n*-butylammonium hexafluorophosphate ($TBAPF_6$) was prepared by metathesis of tetra-*n*-butylammonium iodide with ammonium hexafluorophosphate and was recrystallized three times from ethanol. "Distilled in glass" acetonitrile was purchased from Burdick and Jackson and was used without further purification.

All electrochemical experiments were carried out with a EG&G PAR model 173 potentiostat/galvanostat in conjunction with a EG&G PAR model 175 programmer. Cyclic voltammograms were recorded on a Yokogama 3023 *X*−*Y* recorder. Cyclic voltammetry was performed under nitrogen in a two-compartment cell using a 2 mm diameter platinum disk as the working electrode, a coiled platinum wire as the counter electrode, and an SSCE as the reference electrode. Bulk

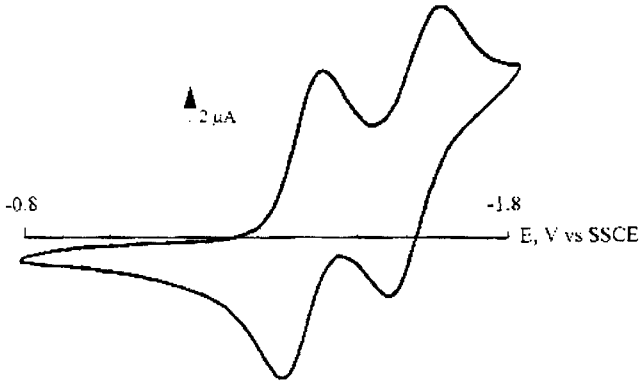

Figure 2. Cyclic voltammogram of L_5, taken in 0.1 M $TBAPF_6$/acetonitrile; platinum working electrode; scan rate = 50 mV/s.

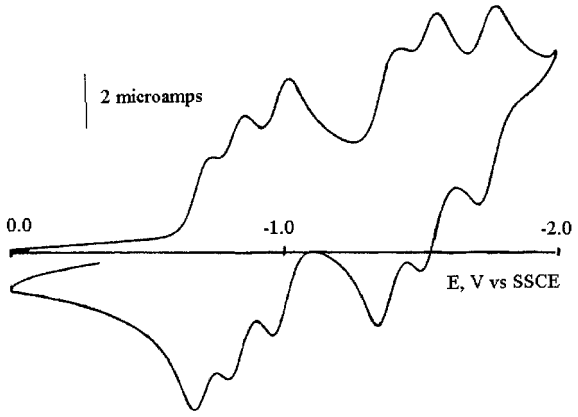

Figure 3. Cyclic voltammogram of $Ru(L_5)_3(PF_6)_2$, taken in 0.1 M $TBAPF_6$/acetonitrile; platinum working electrode; scan rate = 50 mV/s.

electrolysis experiments employed a three-compartment cell, using a 1 cm^2 platinum grid in the middle compartment as the working electrode and a platinum grid (2 cm^2) counter electrode and an SSCE reference electrode in each of the other two compartments. The bulk electrolysis experiments were performed to determine chromophoric properties of the complexes in each oxidation state (2+, 1+, 0, 1-, 2-, etc.). Obtaining each ligand-based reduction state in a completely pure form is impossible due to the proximity in potential of adjacent redox processes for these complexes (the difference in $E_{1/2}$ between successive reductions is less than 150 mV for each complex of this series, thus significant disproportionation occurs; cf. the cyclic voltammogram in Figure 3). The predominance of a redox species (≥80%) is, however, obtained by applying a potential midway between consecutive formal potentials. Consequently, applying these potentials to vigorously stirred solutions of each complex allowed for rapid and optimized generation of the maximum relative amounts of each formal oxidation state species. The visual observation of the colored solutions was performed after the solutions had reached thermodynamic equilibrium (electrochemical currents less than 1% of the initial current).

Results and Discussion

Preparation of the Complexes. The synthesis and characterization of the ligands was straightforward. $Ru(L_1)_3$, $Ru(L_2)_3$, $Ru(L_3)_3$, $Ru(L_4)_3$, and $Ru(L_5)_3$ also were prepared and isolated in pure form as their PF_6^- salts. The lack of success in preparing $Ru(L_6)_3$ is, in retrospect, not surprising. Noncyclic imides are notoriously reactive, particularly to nucleophilic attack at the nitrogen. Under conditions that are required to initiate ligand exchange at the inert Ru(II) center, L_6 likely degrades.

Electrochemistry of the Free Ligands and Corresponding Ruthenium Complexes. The $E_{1/2}(L^{0/-1})$ values obtained from cyclic voltammetry experiments were used to assess the electron-withdrawing strength of each substituent on the bipyridine. Under the conditions used (acetonitrile, 0.1 M $TBAPF_6$; platinum working electrode; scan rate of 50 mV/s), the series of compounds displayed good chemical reversibility. The cyclic voltammograms of L_5 and $Ru(L_5)_3(PF_6)_2$ are displayed in Figures 2 and 3, respectively. The cyclic voltammograms of the other compounds of this study are included as Supporting Information (except for $Ru(L_1)_3$ which has been reported previously[4a]). In the case of L_1 and L_5, the second one-electron reduction of the bipyridine was observed, whereas it was not observed within the solvent window for the other ligands. The reduction potentials are reported in Table 1. Also presented in this table are the Hammett constant values for these substituents.[8] The electronic influence of a substituent X can be estimated by comparing the K_a of substituted benzoic acid (with X either in the para position or the meta position) with the K_a of unsubstituted benzoic acid.[9] Many substituents have been assigned two parameters σ_{meta} and σ_{para}, which are defined by $\sigma_{meta} = \log(K_{Xmeta}/K_0)$ and $\sigma_{para} = \log(K_{Xpara}/K_0)$, where K_{Xmeta} and K_{Xpara} are the acid dissociation constants of the meta-substituted and para-substituted benzoic acid, respectively, and K_0 is the dissociation constant of unsubstituted benzoic acid. Electron-withdrawing substituents increase the dissociation constant and thus have positive σ values, while electron-donating ones decrease the dissociation constant and have negative σ values.

TABLE 1: Electrochemical Data and Hammett Constant Values for a Selection of Substituted 2,2′-Bypyridines

ligand	$E_{1/2}(L^{0/-1})$ V vs SSCE	$E_{1/2}(L^{-1/-2})$ V vs SSCE	σ_{meta}[a]	σ_{para}[a]
2,2′-Bpy	−2.10		0.00	0.00
5,5′-DMBpy	−2.29		−0.07	−0.17
L_1	−1.28	−1.67	0.37	0.45
L_2	−1.81		0.35	0.36
L_3	−1.71			
L_4	−1.30		0.56	0.66
L_5	−1.39	−1.62	0.38	0.50
L_6	−1.27			

[a] Taken from ref 21.

For these bipyridine ligands and complexes, in the electrochemical context, the distinction between para and meta positions is not as significant as it is in the case of benzoic acid dissociation. Even with the substituents in the 5- and 5′-positions, the reaction of interest (injection of an electron in the π^* orbital of the bipyridine) is not localized at a specific site of the ring system, as it is in the benzoic acid ionization case. In an attempt at drawing a linear correlation between $E_{1/2}(L^{0/1-})$ and σ, a slightly better regression was obtained when using σ_p ($r^2 = 0.901$) as compared to σ_m ($r^2 = 0.845$) (see Figure 4). However, in both cases, the fits are fairly poor and it is more appropriate to look at the trends in a qualitative way. Considering the σ values for the amide substituents, it is surprising that they are much harder to reduce than the ester analogue [$E_{1/2}(L_2{}^{0/1-}) = -1.81$ V vs $E_{1/2}(L_1{}^{0/1-}) = -1.28$ V]. The difference between the diethylamide and the methylphenylamide was expected and can be explained as follows. The π-system of the phenyl ring provides some additional delocalization pathway for the amide nitrogen lone pair in L_3. This, in turn, leaves the amide carbonyl with more electron-withdrawing strength toward the pyridine ring, thus making it easier to reduce. The same effect can be observed with the imide-substituted bipyridine (L_6), where the additional carbonyl function bound to the nitrogen makes the carbonyl α to the pyridine ring even more electron withdrawing. This imide ligand is, within

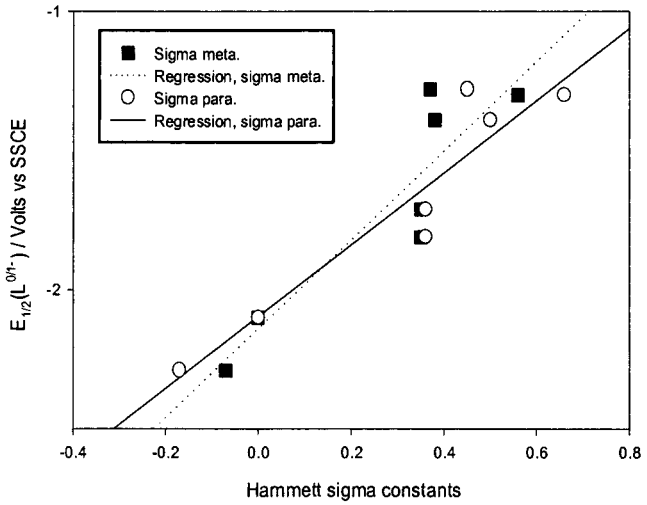

Figure 4. Correlation between the first reduction potential of the free ligands and the Hammett σ constants. Regression coefficients: σ_{meta}, $r^2 = 0.845$; σ_{para}, $r^2 = 0.901$.

TABLE 2: Electrochemical Data for a Series of Ruthenium Trisbipyridine Complexes

ligand	$E_{1/2}(L^{0/-1})$ V vs SSCE	$E_{1/2}[Ru^{2+/1+}(L)_3]$ V vs SSCE	$\lvert\Delta(E_{1/2}s)\rvert$ V
2,2′-Bpy	−2.10	−1.27	0.83
5,5′-DMBpy	−2.29	−1.41	0.88
L1	−1.28	−0.66	0.62
L2	−1.81	−0.98	0.83
L3	−1.71	−0.93	0.78
L4	−1.30	−0.81	0.49
L5	−1.39	−0.70	0.69

experimental error, as easy to reduce as the ester analogue, and its corresponding ruthenium complex, had it been successfully prepared, would have been interesting to characterize. The fact that the imide ligand is easier to reduce than the ketone probably originates from the fact that the alkyl substituent β to the pyridine ring (in L_5) is σ-donating, whereas in L_6, the "amide" group β to the pyridine ring is σ-accepting.

In view of the σ values of cyano groups, the nitrile-substituted bipyridine (L_4) is surprisingly "hard" to reduce. The cyano group is a very strong σ acceptor and somewhat of a weaker π acceptor.[10,11] These observations in conjunction with the better regression using σ_{para} tend to demonstrate that the dominant factor on the value of $E_{1/2}(L^{0/1-})$ is more a delocalization effect than an inductive one.

As for the free ligands, the redox potentials of the ligand-based reductions of the ruthenium complexes, $E^{1/2}[Ru(L)_3^{2+/1+}]$, were determined by cyclic voltammetry. These values, as well as the $E_{1/2}$ values of the free ligands reduction, are listed in Table 2. $Ru(L_1)_3$, $Ru(L_2)_3$, $Ru(L_3)_3$, $Ru(L_4)_3$ and $Ru(L_5)_3$ display reversible electrochemistry, with only the first set of three one-electron reductions being accessible for $Ru(L_2)_3$ and $Ru(L_3)_3$ because of the potential window of acetonitrile. The six ligand-based one-electron reductions (two sets of three) are observable for $Ru(L_1)_3$, $Ru(L_4)_3$, and $Ru(L_5)_3$. Noticeably, there is a small potential separation between the two sets of three waves for $Ru(L_5)_3$. Most probably, this is caused by the small potential separation between the two reductions of the free ketone ligand (i.e., 230 mV for L_5 compared to 390 mV for L_1).

As with the free ligands, attempts at drawing a linear correlation between $E_{1/2}[Ru(L)_3^{2+/1+}]$ and the Hammett constants of the substituents on the bipyridines yielded poor results ($r^2 = 0.851$). However, as can be seen in Figure 5, there is a good linear correlation between $E_{1/2}[Ru(L)_3^{2+/1+}]$ and $E_{1/2}(L^{0/1-})$ ($r^2 = 0.947$, slope = 0.69). This correlation is greatly improved ($r^2 = 0.989$, slope = 0.76) if the data point of the nitrile-substituted ligand (L_4) is not taken into account. The reduction potentials of the complexes are more positive than those of their respective free ligands. This indicates that, in each complex, the reduced radical anion is a better ligand and thus bound more tightly than its neutral counterpart.[4a] The larger the difference between the $Ru(L)_3^{2+/1+}$ and $L^{0/1-}$ reduction potential, the larger is the binding energy preference of Ru(II) for $L^{-\bullet}$ over L. The slope of the line in Figure 4 is less than unity, and this fact provides some subtle insight into the mode of binding in these complexes. The main contribution comes from σ donation from the bipyridines' nitrogen lone pairs, but also involved is the π-back-bonding provided by the π-antibonding orbital of the ligands. The fact that the difference between $E_{1/2}[Ru(L)_3^{2+/1+}]$ and $E_{1/2}[L^{0/1-}]$ decreases as $E_{1/2}[L^{0/1-}]$ becomes more positive tends to prove that the injection of an electron in the bound ligand decreases its π-back-bonding ability more than it improves its σ-donating ability.[4a] This trend is even more accentuated in the case of the cyano-substituted bipyridine (L_4). As can be seen in Table 2, $\Delta E_{1/2}$s for L_4 (i.e., the difference between $E_{1/2}[Ru(L_4)_3^{2+/1+}]$ and $E_{1/2}[L_4^{0/1-}]$) is smaller than expected from the linear trend defined by the other entries in the table. This is consistent with the fact that the cyano group is much more of a σ-acceptor than a π-acceptor. The added electron in the bipyridine does not improve the σ-donating ability of this ligand as much as it does for the other bipyridines considered, as a result of the strong attractive inductive effect of the cyano group which lowers, to some extent, the electron density on the ring.

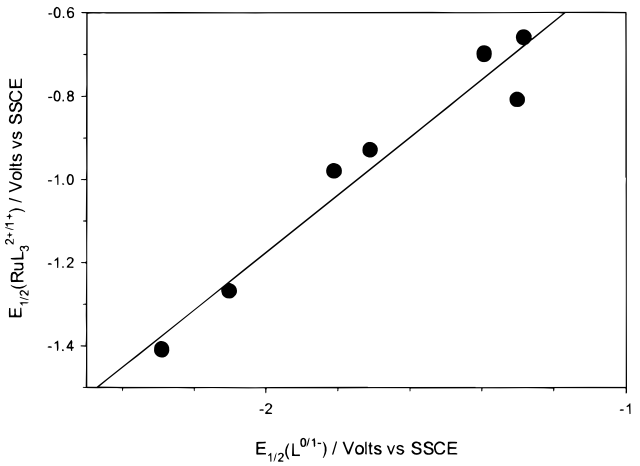

Figure 5. Correlation between the first reduction potential of selected free ligands with the first ligand-based reduction potential of the corresponding ruthenium tris complex. The ligands included are 5,5′-dimethyl-2,2′-bipyridine, 2,2′-bipyridine, L_1, L_2, L_3, L_4, and L_5.

Electrochromic Behavior of $Ru(L_1)_3$, $Ru(L_2)_3$, $Ru(L_3)_3$, $Ru(L_4)_3$, and $Ru(L_5)_3$. The next goal of this study was to evaluate the effect that different substitution in the 5- and 5′ -positions of the bipyridine had on the electrochromic properties of the corresponding ruthenium complexes. Bulk electrolysis was, thus, performed on each of the compounds. By applying potentials which maximized the concentration of each single redox species and letting the solution reach equilibrium, one can visually observe the color of the species in solution. As displayed in Table 3, all complexes synthesized displayed some pleasant electrochromism. The color ranges of the new complexes, however, are not as wide as that for $Ru(L_1)_3$ and the colors are not as sharply defined.[4a] The 2− and 3− oxidation states of

TABLE 3: Visual Observation of the Electrochromic Behavior of Selected Ruthenium Complexes

formal RuL_3 redox state	L_1	L_2	L_3	L_4	L_5
+2	orange	orange	orange	red−orange	red−orange
+1	purple	wine red	gray−blue	purple	red−brown
0	blue	purple	turquoise	blue	purple−brown
−1	green	blue	green	turquoise	gray−blue
−2	brown			aquamarine	green
−3	red			brown−green	purple

$Ru(L_2)_3$ and $Ru(L_3)_3$ could not be accessed, once again, because of the potential window of the solvent.

Conclusion

Five new and one previously known bipyridine ligands containing electron-withdrawing groups in the 5- and 5′-positions of the rings have been synthesized. With one exception, their corresponding ruthenium tris complexes were also synthesized. A rough linear correlation between the reduction potentials of the free ligands and the Hammett constants of the electron-withdrawing groups has been established. A much better linear correlation between the potential of the first reduction of the free ligands and the first ligand-based reduction potential of the corresponding ruthenium tris complexes was found. The cyano-substituted ligand fits this correlation much more poorly than the rest. Most likely, this difference arises from the fact that cyano groups are much better σ-acceptors than they are π-acceptors; thus, their effect on the ligand π^*-orbital is smaller and less direct than those of the other substituents considered here. All of the ruthenium complexes synthesized display some multicolor electrochromism, but none were superior in this regard to the previously studied complex $Ru(L_1)_3$.

Acknowledgment. Support of this work by the National Science Foundation (CHE-971408) is gratefully acknowledged.

Supporting Information Available: Cyclic voltammograms of selected compounds shown in Figure 1 and their ruthenium complexes. This material is available free of charge via the Internet at http://pubs.acs.org.

References and Notes

(1) Juris, A.; Balzani, V.; Barigeletti, F.; Campagna, S.; Belser, P.; Von Zelewsky, A. *Coord. Chem. Rev.* **1988**, *84*, 85.

(2) Abruña, H. D.; Bard, A. J. *J. Am. Chem. Soc.* **1982**, *104*, 2641.

(3) Elliott, C. M.; Pichot, F.; Bloom, C. J.; Rider, L. S. *J. Am. Chem. Soc.* **1998**, *120*, 6781.

(4) (a) Elliott, C. M.; Hershenhart, E. J. *J. Am. Chem. Soc.* **1982**, *104*, 7519. (b) While their electrochemistry is similar, the spectral behaviors of $Ru(L_1)_3$ and its analogue substituted in the 4- and 4′-positions are quite different. Complete spectra of these two complexes are presented in ref 4a along with a discussion of their differences.

(5) Elliott, C. M. *J. Chem. Soc., Chem. Commun.* **1980**, 261.

(6) March, J. *Advanced Organic Chemistry*, 3rd ed.; John Willey & Sons: New York, 1985; pp 932−933.

(7) Posner, G. H.; Whitten, C. E.; McFarland, P. E. *J. Am. Chem. Soc.* **1972**, *94*, 5106.

(8) Hansch, C.; Leo, A.; Unger, S. H.; Kim, K. H.; Nikaitani, D.; Lien, E. J. *J. Med. Chem.* **1973**, *16*, 1207.

(9) Hammett, L. P. *J. Am. Chem. Soc.* **1937**, *59*, 96.

(10) Swain, C. G.; Lupton, E. C. *J. Am. Chem. Soc.* **1968**, *90*, 4328.

(11) Bromilow, J.; Brownlee, R. T. C.; Lopez, V. O.; Taft, R. W. *J. Org. Chem.* **1979**, *44*, 4766.